Draft version November 20, 2025
Typeset using LaTeX **twocolumn** style in AASTeX7.0.1

Cosmological constraints on nonphantom dynamical dark energy with DESI Data Release 2 Baryon Acoustic Oscillations: A 3σ+ lensing anomaly

Shouvik Roy Choudhury,[1] Teppei Okumura,[1,2] and Keiichi Umetsu[1]

[1] *Institute of Astronomy and Astrophysics, Academia Sinica, No. 1, Section 4, Roosevelt Road, Taipei 106319, Taiwan*
[2] *Kavli Institute for the Physics and Mathematics of the Universe (WPI), UTIAS, The University of Tokyo, Chiba 277-8583, Japan*

(Received; Revised; Accepted; Published)

ABSTRACT

We consider a 12-parameter cosmological model with non-phantom dynamical dark energy (NPDDE), where non-phantom implies that the equation of state (EoS) of dark energy (DE), $w(z) \geq -1$ for all redshifts z. Thus, the DE-EoS covers the parameter space corresponding to the popular single scalar-field dark energy models, i.e., Quintessence. The cosmological model comprises 6 parameters of the Λ-Cold Dark Matter (ΛCDM) model, and additionally the dynamical DE EoS parameters (w_0, w_a), the scaling of the lensing amplitude ($A_{\rm lens}$), sum of the neutrino masses ($\sum m_\nu$), the effective number of non-photon relativistic degrees of freedom ($N_{\rm eff}$), and the running of the scalar spectral index (α_s). We derive constraints on the parameters by combining the latest Dark Energy Spectroscopic Instrument (DESI) Data Release (DR) 2 Baryon Acoustic Oscillation (BAO) measurements with cosmic microwave background (CMB) power spectra from Planck Public Release (PR) 4, CMB lensing data from Planck PR4 and Atacama Cosmology Telescope (ACT) DR6, uncalibrated Type Ia supernovae (SNe) data from the Pantheon+ and Dark Energy Survey (DES) Year 5 (DESY5) samples, and Weak Lensing (WL) data from DES Year 1. Our major finding is that with CMB+BAO+WL and CMB+BAO+SNe+WL, we find 3σ+ evidence for $A_{\rm lens} > 1$ even with Planck PR4, indicating a higher than expected CMB lensing amplitude relative to the NPDDE prediction of unity. This implies that for cosmology to accommodate realistic quintessence-like dark energy models (as opposed to unrealistic phantom DE), one would also need to explain a relatively significant presence of the lensing anomaly.

1. INTRODUCTION

The nature of dark energy (DE) remains one of the central open questions in modern cosmology. The Λ-Cold Dark Matter (ΛCDM) model has achieved remarkable success in accounting for a wide array of cosmological observations across both low and high redshifts. However, recent results from the Dark Energy Spectroscopic Instrument (DESI) collaboration Adame et al. (2024a,b); Abdul Karim et al. (2025); Lodha et al. (2025b) have provided intriguing hints for an evolving dark energy component, including a possible phantom crossing around redshift $z \simeq 0.5$ when analyzed with several commonly used parameterizations of dynamical dark energy Lodha et al. (2025b). When combined with Cosmic Microwave Background (CMB) and Type Ia supernovae (SNe Ia) data, the DESI Data Release (DR) 2 measurements of Baryon Acoustic Oscillations (BAO) disfavor the cosmological constant at the level of 2.8σ, 3.8σ, and 4.2σ, depending on the supernovae (SNe) compilation employed—PantheonPlus Brout et al. (2022), Union3 Rubin et al. (2023a), and Dark Energy Survey (DES) Year 5 (DESY5) Abbott et al. (2024), respectively. These results were obtained within an eight-parameter cosmological model using the Chevallier-Polarski-Linder (CPL) parameterization Chevallier & Polarski (2001); Linder (2003) of the dark energy equation of state (EoS), defined as

$$w(z) \equiv w_0 + w_a \frac{z}{1+z}, \qquad (1)$$

where z is the redshift. The potentially far-reaching implications of these findings have triggered an extensive wave of follow-up investigations into the physics of dark energy (see e.g., Roy Choudhury & Okumura 2024; Roy Choudhury 2025; Tada & Terada 2024; Berghaus et al. 2024; Park et al. 2024; Yin 2024; Shlivko & Steinhardt 2024; Cortês & Liddle 2024; Lodha et al. 2025a; Carloni et al. 2025; Croker et al. 2024; Mukherjee & Sen

Email: sroy@asiaa.sinica.edu.tw

2024; Roy 2025; Wang & Piao 2024; Gialamas et al. 2025a; Orchard & Cárdenas 2024; Giarè et al. 2024; Dinda & Maartens 2025a; Jiang et al. 2024; Rebouças et al. 2025; Bhattacharya et al. 2024; Pang et al. 2025; Ramadan et al. 2024; Wolf et al. 2024; Efstathiou 2025; Kessler et al. 2025; Gao et al. 2025b; Borghetto et al. 2025; Wolf et al. 2025c; Huang et al. 2025; Peng & Piao 2025; Tsedrik et al. 2025; Reeves et al. 2025; Yang et al. 2025b; Park & Ratra 2025a; Odintsov et al. 2025; Shim et al. 2025; Gao et al. 2025a; Payeur et al. 2025; Ye 2024; Luongo & Muccino 2025; Wolf et al. 2025b; Giarè 2025; Chakraborty et al. 2025; Elbers et al. 2025; Giarè et al. 2025; Wolf & Read 2025; Ye & Cai 2025; Colgáin et al. 2026; Colgáin et al. 2025; Ye et al. 2025; Silva et al. 2025; Park et al. 2025; Luciano & Paliathanasis 2025; Fazzari et al. 2025; Zhou et al. 2025; Wu et al. 2025; van der Westhuizen et al. 2025b,c,a; Chen et al. 2025; Barua & Desai 2025; Chaudhary et al. 2025b; Wang et al. 2025b; Feng et al. 2025; Braglia et al. 2025; Li et al. 2025b; Silva & Nunes 2025; Lee et al. 2025; Li et al. 2025c; Mishra et al. 2025; Mazumdar et al. 2025; Liu et al. 2025; Högås & Mörtsell 2025; Giarè et al. 2025; Gialamas et al. 2025b; Özülker et al. 2025; Wang & Piao 2025; Luciano et al. 2026; van der Westhuizen et al. 2025d; Mukherjee & Sen 2025; Moffat & Thompson 2025; Bayat & Hertzberg 2025; Giani et al. 2025; Cheng et al. 2025; Ye & Lin 2025; Jhaveri et al. 2025; Scherer et al. 2025; Dinda & Maartens 2025b; Mirpoorian et al. 2025; Paliathanasis 2025; Kou & Lewis 2025; Dinda et al. 2025; Wolf et al. 2025a; García Escudero et al. 2025; Toomey et al. 2025; Adam et al. 2025; Huang 2025; Sanyal & Rudra 2025; Plaza et al. 2025; Yang 2025; Wang et al. 2025c; Yang et al. 2025a; Petri et al. 2025; Meetei & Singh 2025; Roy & Chakrabarti 2025; Arora et al. 2025; Akita et al. 2025; Ishak & Medina-Varela 2025; Zapata et al. 2025; Chaudhary et al. 2025c; Shah et al. 2025; Guedezounme et al. 2025; Goldstein et al. 2025; Qiang et al. 2025; Sharma et al. 2025; Nojiri et al. 2025; Li & Wang 2025; Herold & Karwal 2025; An et al. 2025; Lee 2025; Wang & Freese 2025; Bhattacharya et al. 2025; Li et al. 2024, 2025a; Chaudhary et al. 2025a; Chakraborty et al. 2024; Hossain & Maqsood 2025).

The line at $w = -1$ (corresponsing to the cosmological constant or Λ) separates the behavior of dark energy into two regimes: phantom ($w < -1$) and non-phantom ($w \geq -1$). In this work, we focus only on the non-phantom scenario and exclude the phantom region. From a quantum field theory standpoint, models with a single scalar field cannot cross the $w = -1$ boundary, while more general models that do allow it require additional degrees of freedom to maintain gravitational stability. Theories that accommodate phantom dark energy typically suffer from issues such as Lorentz violation, unstable vacuum, superluminal modes, ghosts, non-locality, or instability to quantum corrections (Caldwell et al. 2003; Nesseris & Perivolaropoulos 2004; Vikman 2005; Fang et al. 2008). On the other hand, single scalar field models like quintessence are theoretically well motivated, avoid these problems, and remain strictly non-phantom (Linder 2008; Caldwell & Linder 2005; Zlatev et al. 1999; Wang & Tegmark 2004). Therefore, in this work we restrict our analysis to the non-phantom dynamics throughout the evolution of the universe, i.e., w(z) $\geq$-1 for all redshifts z. We, however, emphasize here, that an apparent effective equation of state $w < -1$ can arise without the above mentioned pathologies in more complicated but stable frameworks, such as multi-field dark energy models (Feng et al. 2005; Cai et al. 2010; Guo et al. 2005; Akrami et al. 2021; Eskilt et al. 2022) or in scenarios involving interactions between dark energy and dark matter (Amendola 2000; Farrar & Peebles 2004; van de Bruck et al. 2017).

It should be noted that in the 8-parameter w_0w_aCDM model analyzed by the DESI Collaboration, the non-phantom region of dynamical dark energy is excluded at more than 2σ significance when using CMB+BAO or CMB+BAO+SNe dataset combinations. However, two recent works Roy Choudhury & Okumura (2024); Roy Choudhury (2025) showed that extending the dynamical dark energy framework to a 12-parameter model allows a substantial portion of the non-phantom region to remain consistent within 2σ when using CMB+BAO+Pantheon+. Moreover, in this extended parameter space, the non-phantom region is not conclusively ruled out beyond 2σ by either the CMB+BAO or the CMB+BAO+DESY5 dataset combinations. Therefore, analyzing the non-phantom dynamical dark energy model (hereafter NPDDE) is well motivated in the 12-parameter setup considered in Roy Choudhury & Okumura (2024); Roy Choudhury (2025), though it is disfavored in the minimal 8-parameter w_0w_aCDM model studied by the DESI Collaboration.

The extended model includes the six baseline ΛCDM parameters along with the following extensions: the dynamical dark energy equation of state parameters (w_0, w_a) in the CPL parametrization, the sum of neutrino masses ($\sum m_\nu$), the effective number of relativistic species ($N_{\rm eff}$), the lensing amplitude scaling parameter ($A_{\rm lens}$), and the running of the scalar spectral index (α_s)[3]. For the CMB data, we employ the latest

[3] For previous studies in such largely extended parameter spaces, see Di Valentino et al. (2015, 2016, 2017); Poulin et al. (2018); Roy Choudhury & Naskar (2019); Di Valentino et al. (2020).

Planck Public Release 4 (PR4, 2020) likelihoods, namely HiLLiPoP and LoLLiPoP (Tristram et al. 2024), together with Planck PR4 lensing combined with ACT DR6 lensing likelihoods (Madhavacheril et al. 2024). For BAO, we use the DESI DR2 BAO likelihoods (Abdul Karim et al. 2025), while for supernovae we adopt the most recent uncalibrated Type Ia Supernova likelihoods: Pantheon+ (Brout et al. 2022) and DESY5 (Abbott et al. 2024). In addition, we make use of the Dark Energy Survey Year 1 (DESY1) galaxy clustering and weak lensing data (Abbott et al. 2018)[4].

We now outline the motivation for extending the $w_0 w_a$CDM model (apart from allowing for the NPDDE parameter space). Neutrinos, while massless in the Standard Model, are known from oscillation experiments to be massive, requiring at least two non-zero masses with mass-squared splittings $\Delta m^2_{21} \simeq 7.42 \times 10^{-5}$ eV^2 and $|\Delta m^2_{31}| \simeq 2.51 \times 10^{-3}$ eV^2. This implies two possible mass orderings: Normal ($\sum m_\nu > 0.057$ eV) and Inverted ($\sum m_\nu > 0.096$ eV) (Esteban et al. 2020). Hence, the inclusion of $\sum m_\nu$ represents a simple and well-motivated extension to the baseline model. Dynamical dark energy, parameterized through the CPL form (w_0, w_a), is also relevant since it introduces geometric degeneracies with $\sum m_\nu$ (Roy Choudhury & Hannestad 2020). Notably, the DESI Collaboration has reported that the preferred w_0–w_a region lies in the phantom regime (Adame et al. 2024a,b; Abdul Karim et al. 2025), which relaxes the bounds on $\sum m_\nu$ by more than a factor of two due to the well-known degeneracy between the dark energy equation of state and the neutrino mass (Hannestad 2005). This degeneracy is of significant importance here, as the NPDDE parameter space ($w(z) \geq -1$) prefers lower values of $\sum m_\nu$ than a cosmological constant ($w = -1$), and thus stronger bounds on $\sum m_\nu$ are achieved in a cosmological model with NPDDE than Λ, a fact first noticed in 2018 by Vagnozzi et al. (2018); Roy Choudhury & Naskar (2019); Roy Choudhury & Choubey (2018). Due to this degeneracy, it is expected that the bounds on $\sum m_\nu$ obtained in this paper will be stronger than our recent works Roy Choudhury & Okumura (2024); Roy Choudhury (2025),[5] where the full dynamical DE parameter space was allowed.

Massive neutrinos, upon becoming non-relativistic, suppress the growth of structure on small scales, thereby affecting CMB lensing and enhancing small-scale anisotropy correlations (Roy Choudhury 2020; Lesgourgues & Pastor 2012). The $> 2\sigma$ lensing anomaly in the Planck PR3 (2018) likelihoods ($A_{\rm lens} = 1.18 \pm 0.065$ at 68%) (Aghanim et al. 2020a,b) has essentially disappeared ($< 1\sigma$) in Planck PR4 (Tristram et al. 2024) in the ΛCDM model, which motivates the use of PR4 for robust neutrino mass constraints[6]. Since $\sum m_\nu$ and $A_{\rm lens}$ are correlated, including $A_{\rm lens}$ as a free parameter in combination with Planck PR4 likelihoods helps mitigate potential systematic biases in neutrino mass inference.

We further note that recent studies have identified a correlation between $A_{\rm lens}$ and the dark energy equation of state parameters (Park & Ratra 2025b; Park et al. 2025), which leads to a relaxation of the constraints on w_0 and w_a. A similar relaxation was observed in our earlier works (Roy Choudhury & Okumura 2024; Roy Choudhury 2025). This correlation effectively reduces the apparent tension with ΛCDM (and NPDDE) relative to that reported by the DESI Collaboration (Abdul Karim et al. 2025). However, this reduction in tension comes at the cost of increasing the preferred value of $A_{\rm lens}$, thereby shifting it away from consistency with the canonical value $A_{\rm lens} = 1$. It will be, thus, of great importance to analyse what happens to the $A_{\rm lens}$ parameter (and thus the lensing anomaly) when the parameter space is strictly restricted to the NPDDE region that corresponds to realistic quantum field theories of dark energy. Weak Lensing data can further exacerbate the lensing anomaly, as we noticed in our recent work Roy Choudhury (2025), where we showed for the first time that even with Planck PR4 likelihoods, addition of a non-CMB data like DES Year 1 Weak Lensing with CMB+BAO+SNe can lead to a >2σ lensing anomaly in this 12 parameter model, but with full range of w_0, w_a allowed.

[4] We note that more recent weak lensing data from DES Year 3 are available; however, the corresponding likelihoods have been released only for `CosmoSIS` (Zuntz et al. 2015) and not for `Cobaya` (Torrado & Lewis 2021), which is the MCMC code adopted in this work.

[5] For earlier bounds on $\sum m_\nu$ in the literature, see e.g., Roy Choudhury & Choubey (2018); Roy Choudhury & Hannestad (2020); Tanseri et al. (2022); Vagnozzi et al. (2017, 2018); Roy Choudhury & Naskar (2019); Di Valentino et al. (2021); Giusarma et al. (2018); Reeves et al. (2023); Yang et al. (2017); Roy Choudhury & Choubey (2019). For more recent studies, see Shao et al. (2025); Jiang et al. (2025); Herold & Kamionkowski (2025); Roy Choudhury & Okumura (2024); Bertólez-Martínez et al. (2024); Wang et al. (2025a); Roy Choudhury (2025)

[6] The $A_{\rm lens}$ parameter was first defined in (Calabrese et al. 2008).

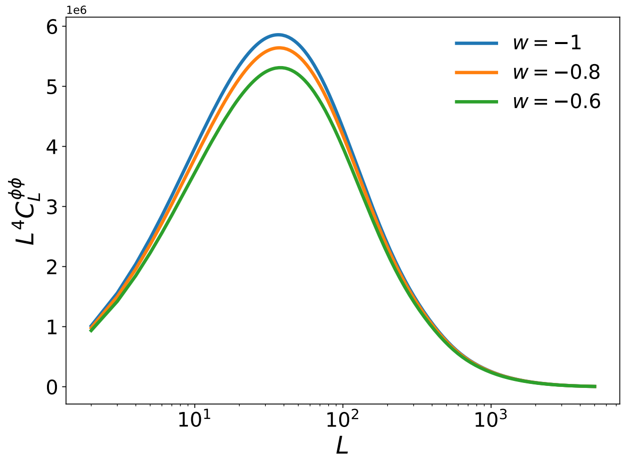

Figure 1. The CMB lensing-potential powerspectrum for different values of the constant DE EoS w. The angular scale of sound horizon at recombination, θ_s^*, is kept fixed by adjusting H_0.

The redshift at which the matter and dark energy densities become equal, denoted by $z_{\rm eq}$, is obtained from the condition $\rho_m(z_{\rm eq}) = \rho_{\rm DE}(z_{\rm eq})$. Assuming a constant dark energy equation of state w, the matter and dark energy densities evolve as $\rho_m(z) = \rho_{m0}(1+z)^3$ and $\rho_{\rm DE}(z) = \rho_{\rm DE,0}(1+z)^{3(1+w)}$, where ρ_{m0} and $\rho_{\rm DE,0}$ are their present-day values. This leads to

$$1 + z_{\rm eq} = \left(\frac{\Omega_{\rm DE,0}}{\Omega_{m0}}\right)^{-1/(3w)}, \tag{2}$$

where Ω_{m0} and $\Omega_{\rm DE,0}$ are the present-day fractional density parameters of matter and dark energy, respectively. For $w = -1$ (the ΛCDM case), Eq. (2) reduces to $1+z_{\rm eq} = (\Omega_{\rm DE,0}/\Omega_{m0})^{1/3}$. Since the exponent $-1/(3w)$ increases as w becomes less negative, non-phantom dark energy models ($w > -1$) yield a higher $z_{\rm eq}$, implying that matter–dark energy equality occurs earlier in cosmic history compared to ΛCDM, for the same value of Ω_{m0}. In contrast, phantom models ($w < -1$) result in a lower $z_{\rm eq}$, meaning that equality occurs later. This earlier onset of dark energy dominance in non-phantom models suppresses the growth of large-scale structure and reduces the amount of CMB lensing relative to ΛCDM. We can visualize this effect in Figure 1, where we have plotted the CMB lensing-potential power spectrum $C_L^{\phi\phi}$ for different values of the constant DE EoS w. The deeper we go into the non-phantom regime larger the suppression of the power spectrum. Thus, a correlation between the DE EoS and $A_{\rm lens}$ is naturally expected and a preference for $A_{\rm lens} > 1$ essentially indicates that the data prefers more CMB lensing than what is theoretically predicted by the non-phantom model.

The scaling of the lensing amplitude $A_{\rm lens}$ is also degenerate with the spatial curvature parameter Ω_k (Di Valentino et al. 2019), linking the lensing anomaly to the preference for a nonzero curvature (Di Valentino et al. 2019; Handley 2021). In particular, Planck PR3 (2018) data alone favored a closed universe ($\Omega_k < 0$), excluding $\Omega_k = 0$ at more than 2σ. This preference for a closed universe, however, vanishes once BAO and supernova datasets are included (Aghanim et al. 2020b). By contrast, the lensing anomaly persisted above 2σ even when these additional datasets were combined with Planck PR3. The DESI Collaboration has likewise reported no significant deviation from flatness in dynamical dark energy models (Abdul Karim et al. 2025), albeit in the ΛCDM+Ω_k model a 2σ+ preference for positive Ω_k is seen Abdul Karim et al. (2025); Chen & Zaldarriaga (2025). Separate studies using physical models for quintessence like exponential quintessence Akrami et al. (2025) or thawing quintessence Dinda & Maartens (2025b) also show a 2σ+ preference for a nonzero positive curvature. However, these last two studies only make use of background data, neglecting the perturbation information encoded in the full CMB measurements. Nevertheless, it may be worthwhile to investigate the role of spatial curvature by allowing the cosmological model to vary in Ω_k. Since MCMC analyses with nonzero Ω_k are computationally expensive, we defer such an exploration to future work. In the present study, we concentrate on the lensing anomaly and therefore fix $\Omega_k = 0$ throughout our analysis, i.e., we restrict ourselves to a spatially flat universe.

Another key motivation arises from the Hubble tension, a $\sim 4.6\sigma$ discrepancy between the local SH0ES measurement ($H_0 = 73.04 \pm 1.04$ km/s/Mpc) (Riess et al. 2022) and the Planck PR4 inference ($H_0 = 67.64 \pm 0.52$ km/s/Mpc) (Tristram et al. 2024) within ΛCDM. This tension may be alleviated by phantom dark energy (Roy Choudhury & Hannestad 2020; Vagnozzi 2020) or by a fully thermalized additional radiation species ($\Delta N_{\rm eff} \sim 1$), although the latter is disfavored by data (Aghanim et al. 2020b; Vagnozzi 2023; Roy Choudhury et al. 2021; Choudhury et al. 2021; Roy Choudhury et al. 2022; Bostan & Roy Choudhury 2024). We nevertheless include $N_{\rm eff}$ as a free parameter to test the extent to which the H_0 tension can be reduced in a 12-parameter framework, even if we do not expect to fully resolve it. A larger $N_{\rm eff}$ increases the pre-recombination expansion rate, which in turn raises the inferred value of H_0. Given the significance of the Hubble tension in contemporary cosmology, we consider varying $N_{\rm eff}$ an essential extension.

Finally, we include the running of the scalar spectral index, α_s. In slow-roll inflationary models, one typically expects $\log_{10}|\alpha_s| \sim -3.2$ (Garcia-Bellido & Roest 2014), though alternative inflationary scenarios can produce significantly larger deviations (see, e.g., Easther & Peiris (2006); Kohri & Matsuda (2015); Chung et al. (2003)). Allowing α_s to vary enables us to test for such possible departures from the standard slow-roll expectation.

Beyond our general motivation to constrain the parameters of a cosmological model with NPDDE, the primary goals of this paper are threefold:

1. To further investigate the lensing anomaly (or $A_{\rm lens}$ anomaly) in the 12-parameter NPDDE framework, particularly in the presence of weak lensing data.

2. To re-assess the bounds on $\sum m_\nu$ in an NPDDE model using the new DESI DR2 BAO likelihoods.

3. To examine the robustness of the Hubble tension (Riess et al. 2022; Knox & Millea 2020; Banerjee et al. 2021; Lee et al. 2022) in this significantly extended parameter space.

With the release of DESI DR2 BAO data, we consider this an opportune moment to revisit and update the constraints in an extended cosmological model with non-phantom dark energy. The resulting constraints are expected to be of considerable relevance to both the cosmology and particle physics communities.

The remainder of the paper is organized as follows. Section 2 describes the analysis methodology. Section 3 presents and discusses the results of our statistical analysis. Finally, Section 4 summarizes our conclusions.

2. ANALYSIS METHODOLOGY

In Section 2.1, we describe the cosmological model, the parameter sampling and plotting codes, and the priors adopted for the parameters. Section 2.2 provides an overview of the cosmological datasets employed in this work.

2.1. *Cosmological model and parameter sampling*

Here is the parameter vector for this extended model with 12 parameters :

$$\theta \equiv \Big[\omega_c,\ \omega_b,\ \Theta^*_s,\ \tau,\ n_s,\ \ln(10^{10}A_s), w_{0,\rm DE}, w_{a,\rm DE}, N_{\rm eff}, \sum m_\nu, \alpha_s, A_{\rm lens}\Big]. \quad (3)$$

The first six parameters correspond to the standard ΛCDM model: the present-day cold dark matter energy density, $\omega_c \equiv \Omega_c h^2$; the present-day baryon energy density, $\omega_b \equiv \Omega_b h^2$; the reionization optical depth, τ; the scalar spectral index, n_s; and the amplitude of the primordial scalar power spectrum, A_s (both evaluated at the pivot scale $k_* = 0.05$ Mpc^{-1}). Additionally, Θ^*_s denotes the ratio of the sound horizon to the angular diameter distance at the epoch of photon decoupling.

The remaining six parameters extend the ΛCDM framework. For the CPL parametrization of the dark energy equation of state, we use the notation $(w_{0,\rm DE}, w_{a,\rm DE})$ interchangeably with (w_0, w_a). The other extended parameters, as discussed in the Introduction, include the effective number of non-photon relativistic species ($N_{\rm eff}$), the sum of neutrino masses ($\sum m_\nu$), the running of the scalar spectral index (α_s), and the lensing amplitude scaling parameter ($A_{\rm lens}$).

Here, given equation (1), $w(z=0) = w_{0,\rm DE}$ denotes the present-day dark energy equation of state (EoS), while $w(z\to\infty) = w_{0,\rm DE} + w_{a,\rm DE}$ corresponds to its value in the early universe. The function $w(z)$ evolves monotonically between these two limits. Consequently, in order to restrict the analysis to the NPDDE region of parameter space, i.e., $w(z) \geq -1$, it suffices to impose the hard priors

$$w_{0,\rm DE} \geq -1, \qquad w_{0,\rm DE} + w_{a,\rm DE} \geq -1. \quad (4)$$

We adopt a degenerate hierarchy for neutrino masses, where all three neutrinos have equal masses, $m_i = \sum m_\nu/3$ for $i = 1,2,3$, and impose a prior $\sum m_\nu \geq 0$. This choice is well motivated, as cosmological observations primarily constrain the total neutrino mass through its impact on the energy density Lesgourgues & Pastor (2012), and even future cosmological data are expected to remain insensitive to the small mass splittings Archidiacono et al. (2020). Moreover, forecasts indicate that assuming a degenerate hierarchy introduces only a negligible bias in the event of a detection of $\sum m_\nu$ Archidiacono et al. (2020). Currently, no compelling evidence favors a particular neutrino mass hierarchy, even when combining cosmological constraints with terrestrial experiments such as neutrino oscillation and beta decay measurements Gariazzo et al. (2022).

Since we allow for a nonzero running of the scalar spectral index, $\alpha_s \equiv dn_s/d\ln k$, with k the wave number, we adopt a standard running power-law model for the primordial scalar power spectrum, given by

$$\ln \mathcal{P}_s(k) = \ln A_s + (n_s - 1)\ln\left(\frac{k}{k_*}\right) + \frac{\alpha_s}{2}\left[\ln\left(\frac{k}{k_*}\right)\right]^2. \quad (5)$$

Small values of $\log_{10}|\alpha_s| \simeq -3.2$ naturally arise in slow-roll inflationary models Garcia-Bellido & Roest

Parameter	Prior
$\Omega_{\rm b}h^2$	[0.005, 0.1]
$\Omega_{\rm c}h^2$	[0.001, 0.99]
τ	[0.01, 0.8]
n_s	[0.8, 1.2]
$\ln(10^{10}A_s)$	[1.61, 3.91]
Θ_s^*	[0.5, 10]
$w_{0,\rm DE}$	[-1, -0.33]
$w_{a,\rm DE}$	[-2, 2]
$N_{\rm eff}$	[2, 5]
$\sum m_\nu$ (eV)	[0, 5]
α_s	[-0.1, 0.1]
$A_{\rm lens}$	[0.1, 2]

Table 1. Flat priors on the main cosmological parameters constrained in this paper.

(2014), although certain inflationary scenarios can produce larger values (see, e.g., Easther & Peiris (2006); Kohri & Matsuda (2015); Chung et al. (2003)).

Parameter Sampling: For all Markov Chain Monte Carlo (MCMC) analyses presented in this work, we employ the cosmological inference framework `Cobaya` Torrado & Lewis (2021); Torrado & Lewis (2019), with theoretical predictions computed using the Boltzmann solver `CAMB` Lewis et al. (2000); Howlett et al. (2012). When including the combined Planck PR4 + ACT DR6 lensing likelihood, we adopt the high-precision settings recommended by the ACT collaboration.

Chain convergence is assessed using the Gelman-Rubin statistics Brooks & Gelman (1998), ensuring that all chains satisfy the criterion $R - 1 < 0.01$. Parameter constraints and the figures shown in this paper are obtained using `GetDist` Lewis (2019). Broad, uniform priors are imposed on all cosmological parameters, as summarized in Table 1.

2.2. *Datasets*

CMB: Planck Public Release (PR) 4: We make use of the most up-to-date measurements of the Cosmic Microwave Background (CMB) temperature and E-mode polarization power spectra on both large angular scales (low-ℓ) and small angular scales (high-ℓ) from the *Planck* satellite. For the high-ℓ ($30 < \ell < 2500$) TT, TE, and EE spectra, we adopt the latest HiLLiPoP likelihoods, as presented in Tristram et al. (2024). The low-ℓ ($\ell < 30$) EE data are analyzed using the most recent LoLLiPoP likelihoods, also described in Tristram et al. (2024). Both HiLLiPoP and LoLLiPoP are based on the *Planck* Public Release (PR) 4, which corresponds to the latest reprocessing of LFI and HFI observations with the unified NPIPE pipeline. This reprocessing provides an expanded dataset with reduced noise levels and improved cross-frequency consistency Akrami et al. (2020). For the low-ℓ TT data, we employ the Commander likelihood from the *Planck* 2018 release Aghanim et al. (2020b). Throughout this work, we collectively denote this combination of likelihoods as **"Planck PR4."**

CMB lensing: Planck PR4+ACT DR6. CMB experiments also provide measurements of the gravitational lensing potential power spectrum, $C_\ell^{\phi\phi}$, obtained via 4-point functions. In this work, we employ the most recent NPIPE PR4 *Planck* CMB lensing reconstruction Carron et al. (2022), together with the Data Release 6 (DR6) from the Atacama Cosmology Telescope (ACT), version 1.2 Madhavacheril et al. (2024); MacCrann et al. (2024). As recommended by the ACT collaboration, we adopt the high-precision likelihood settings Madhavacheril et al. (2024). For brevity, we refer to this combined dataset as **"lensing"**. We also refer to the **Planck PR4+lensing** combination simply as **"CMB."**

BAO: DESI Data Release (DR) 2.We include the most recent Baryon Acoustic Oscillation (BAO) measurements from Data Release 2 of the Dark Energy Spectroscopic Instrument (DESI) collaboration Abdul Karim et al. (2025) (for comparison with the earlier DR1 results, see Adame et al. (2024a)). The DR2 dataset covers multiple tracers across a wide redshift range: the Bright Galaxy Sample (BGS, $0.1 < z < 0.4$), the Luminous Red Galaxy Sample (LRG, $0.4 < z < 0.6$ and $0.6 < z < 0.8$), the Emission Line Galaxy Sample (ELG, $1.1 < z < 1.6$), the combined LRG and ELG sample in the overlapping range (LRG+ELG, $0.8 < z < 1.1$), the Quasar Sample (QSO, $0.8 < z < 2.1$), and the Lyman-α Forest Sample (Lyα, $1.77 < z < 4.16$). For brevity, we collectively denote this dataset as **"DESI."** Since we are not using any other BAO data, we also often refer to this dataset simply as **"BAO"**.

SNeIa: Pantheon+.We utilize the most recent Type Ia Supernova (SNeIa) luminosity distance measurements from the Pantheon+ compilation Scolnic et al. (2022), comprising 1550 spectroscopically confirmed SNeIa over the redshift range $0.001 < z < 2.26$. For our analysis, we adopt the publicly available likelihood from Brout et al. (2022), which incorporates both statistical and systematic covariance. To reduce the impact of peculiar velocities on the Hubble diagram, this likelihood imposes a cut at $z > 0.01$. Throughout this work, we denote this dataset as **"PAN+"**.

SNeIa: DES Year 5. We employ the luminosity distance measurements from the most recent supernova sample released by the Dark Energy Survey (DES) as part of their Year 5 data release Abbott et al. (2024). This catalog consists of 1635 photometrically classified SNeIa spanning the redshift range $0.1 < z < 1.13$. We denote this dataset as **"DESY5"**.

We note that the PAN+ and DESY5 samples have overlapping supernovae. To avoid double counting, these two datasets are never used together in any single analysis. Also, we do not include the Union3 SNe Ia sample (Rubin et al. 2023b), as the DESI Collaboration has shown that it yields parameter constraints and results intermediate between those obtained from the Pantheon+ and DES Year 5 samples. Thus, employing the Pantheon+ and DES Year 5 samples provides the two extreme cases of interest, and that is sufficient for drawing any conclusions regarding cosmological parameters; and we save valuable computational resources by omitting Union3.

Weak Lensing: DES Year 1. We include the likelihood from the joint analysis of galaxy clustering and weak gravitational lensing based on 1321 deg^2 of *griz* imaging data from the first year of the Dark Energy Survey (Abbott et al. 2018). We refer to this dataset as **"WL"** throughout.

3. NUMERICAL RESULTS

Here we present constraints on the 12-parameter spatially flat ($\Omega_k = 0$) cosmological model, with emphasis on the lensing amplitude parameter, $A_{\rm lens}$. Table 2 provides the full set of marginalized parameter bounds for various combinations of Planck PR4, DESI BAO, supernovae (PAN+ and DESY5), and DES Year 1 weak lensing data.

3.1. $w_{0,\rm DE}$ *and* $w_{a,\rm DE}$

As shown in Figure 2, when the parameter space is restricted to non-phantom dark energy ($w(z) \geq -1$), the combination of CMB (Planck PR+lensing) and BAO (DESI) data is still consistent with the cosmological constant ($w_{0,\rm DE} = -1$, $w_{a,\rm DE} = 0$) within 1σ. The inclusion of Pantheon+ excludes the cosmological constant at 1σ, but it remains allowed within 2σ. In contrast, adding the DES Year 5 supernova dataset to the CMB+BAO combination rules out the cosmological constant at more than 2σ. Therefore, the DESY5 supernova data appear to favor a dynamical dark energy scenario even under the restriction to the non-phantom region of the dark energy equation of state. Addition of WL data has negligible impact on the DE EoS parameter constraints.

3.2. $A_{\rm lens}$

From Table 2, it is clear that the CMB+DESI and the CMB+DESI+SNe (for both PAN+ and DESY5)

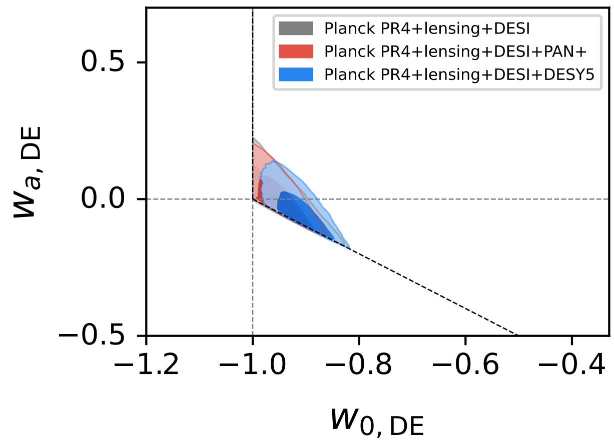

Figure 2. 68% and 95% marginalised contours in the $w_{0,\rm DE} - w_{a,\rm DE}$ plane for different data combinations. The area to the right of the vertical dashed blue line and above the slanted dashed blue line represents the parameter space corresponding to quintessence-like or non-phantom dark energy.

combinations lead to a significant 2σ+ lensing anomaly (i.e. departure from $A_{\rm lens} = 1$). This is in stark contrast to the Planck PR4 Hillipop result in ΛCDM, where the $A_{\rm lens}$-anomaly was reduced to $< 1\sigma$ Tristram et al. (2024). Our result shows for the first time that physically motivated models like Quintessence can lead to a 2σ+ lensing anomaly even with Planck PR4 likelihoods. This can be explained by the correlation between $A_{\rm lens}$ and the DE EoS parameters as recently studied in Park & Ratra (2025a); Park et al. (2025); Roy Choudhury (2025).

The right panel of Figure 3 demonstrates a pronounced negative correlation between S_8 and $A_{\rm lens}$. WL data prefers slightly lower value of S_8 than the CMB+BAO+SNe combination. From the left panel, it is evident that the inclusion of WL data shifts the preferred values of $A_{\rm lens}$ towards even higher values, as expected from this correlation. As reported in Table 2, once WL data are incorporated, the inferred $A_{\rm lens}$ departs from unity at a significance greater than 3σ, which is a significant result. Although residual systematics in the weak lensing reconstruction may play a role, the anomaly could equally well indicate new physics influencing the growth of structure or the lensing potential, particularly if the data are interpreted at face value. An important implication is that if the underlying cosmological model corresponds to a QFT-realistic scenario such as quintessence, it must also account for the presence of a significant lensing anomaly and explain its origin.

Parameter	Planck PR4 + lensing +DESI	Planck PR4 +lensing + DESI + PAN+	Planck PR4 +lensing + DESI + DESY5	Planck PR4 + lensing + DESI + WL	Planck PR4 + lensing+ DESI + PAN+ + WL	Planck PR4 + lensing+ DESI + DESY5 + WL
$\Omega_b h^2$	0.02263 ± 0.00018	0.02264 ± 0.00017	0.02266 ± 0.00017	0.02266 ± 0.00018	0.02265 ± 0.00018	0.02268 ± 0.00017
$\Omega_c h^2$	0.1197 ± 0.0028	0.1197 ± 0.0028	0.1198 ± 0.0028	0.1187 ± 0.0028	0.1187 ± 0.0027	0.1188 ± 0.0027
τ	0.0590 ± 0.0066	0.0591 ± 0.0066	0.0591 ± 0.0066	0.0583 ± 0.0065	0.0584 ± 0.0065	0.0585 ± 0.0065
n_s	0.983 ± 0.008	0.983 ± 0.008	0.984 ± 0.008	0.983 ± 0.008	0.983 ± 0.008	0.984 ± 0.008
$\ln(10^{10} A_s)$	3.044 ± 0.016	3.044 ± 0.016	3.044 ± 0.016	3.040 ± 0.016	3.044 ± 0.016	3.044 ± 0.015
$100\Theta_s^*$	1.04077 ± 0.00038	1.04077 ± 0.00037	1.04077 ± 0.00038	1.04085 ± 0.00038	1.04085 ± 0.00038	1.04085 ± 0.00038
$\sum m_\nu$ (eV)	< 0.161 (2σ)	< 0.163 (2σ)	< 0.153 (2σ)	< 0.199 (2σ)	< 0.196 (2σ)	< 0.186 (2σ)
$N_{\rm eff}$	3.26 ± 0.18	3.27 ± 0.18	3.28 ± 0.18	3.24 ± 0.18	3.24 ± 0.18	3.25 ± 0.18
w_0	< -0.874	$-0.946^{+0.025}_{-0.037}$	-0.910 ± 0.033	< -0.877	$-0.946^{+0.025}_{-0.037}$	-0.910 ± 0.033
w_a	$0.007^{+0.058}_{-0.073}$	$0.006^{+0.043}_{-0.079}$	$-0.039^{+0.039}_{-0.075}$	$0.011^{+0.057}_{-0.074}$	$0.006^{+0.045}_{-0.078}$	$-0.039^{+0.039}_{-0.075}$
α_s	0.0008 ± 0.0071	0.0009 ± 0.0071	0.0013 ± 0.0071	0.0020 ± 0.0071	0.0018 ± 0.0071	0.0022 ± 0.0071
$A_{\rm lens}$	$1.092^{+0.039}_{-0.045}$ (1σ), $1.092^{+0.090}_{-0.080}$ (2σ), $1.092^{+0.12}_{-0.10}$ (3σ)	$1.093^{+0.038}_{-0.046}$ (1σ), $1.093^{+0.085}_{-0.082}$ (2σ), $1.093^{+0.12}_{-0.10}$ (3σ)	$1.098^{+0.038}_{-0.045}$ (1σ), $1.098^{+0.087}_{-0.078}$ (2σ), $1.098^{+0.12}_{-0.10}$ (3σ)	$1.112^{+0.038}_{-0.045}$ (1σ), $1.112^{+0.087}_{-0.077}$ (2σ), $1.112^{+0.12}_{-0.098}$ (3σ)	$1.111^{+0.037}_{-0.044}$ (1σ) $1.111^{+0.086}_{-0.076}$ (2σ), $1.111^{+0.12}_{-0.098}$ (3σ)	$1.113^{+0.037}_{-0.043}$ (1σ), $1.113^{+0.085}_{-0.075}$ (2σ), $1.113^{+0.11}_{-0.097}$ (3σ)
H_0 (km/s/Mpc)	68.5 ± 1.1	68.44 ± 0.96	67.91 ± 0.96	68.5 ± 1.1	68.32 ± 0.98	67.79 ± 0.97
S_8	$0.799^{+0.015}_{-0.012}$	$0.799^{+0.015}_{-0.012}$	$0.800^{+0.015}_{-0.012}$	$0.790^{+0.014}_{-0.012}$	$0.790^{+0.014}_{-0.011}$	$0.791^{+0.014}_{-0.011}$

Table 2. Bounds on cosmological parameters in the 12 parameter extended model. Unless otherwise specified, marginalized limits are given at 68% C.L. whereas upper limits are given at 95% C.L. Note that H_0 and S_8 are derived parameters.

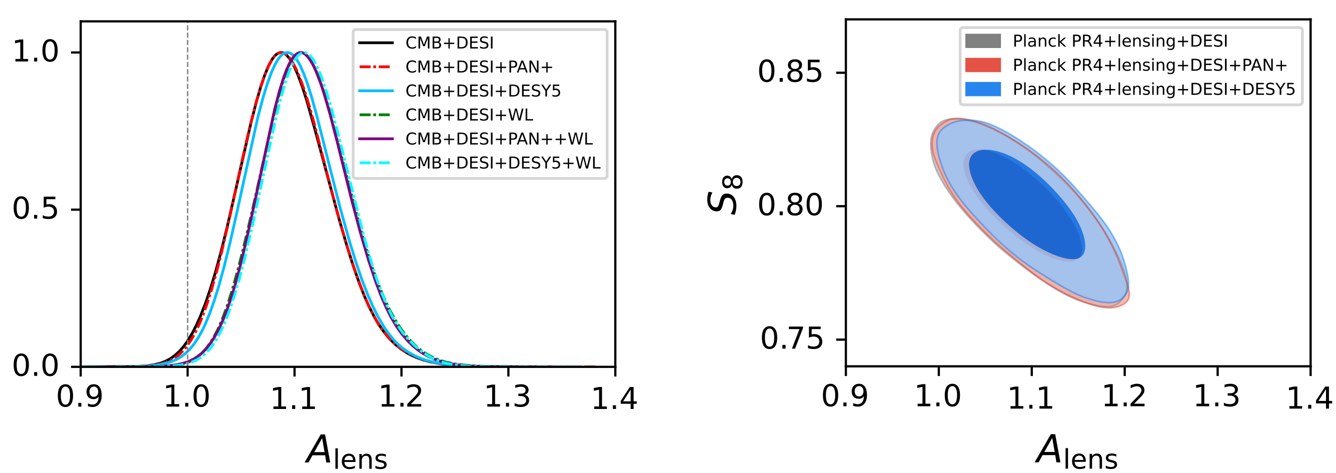

Figure 3. The left panel shows the 1D posterior distributions of $A_{\rm lens}$ for various data combinations. The right panel shows its 2D correlation plots with the S_8 parameter. We note that dataset combinations with WL included leads to a $3\sigma+$ lensing anomaly due to the strong negative correlation with S_8. Even without the WL data, the lensing anomaly is $2\sigma+$.

We note that the DES Year 1 WL data used in this analysis yields $S_8 = 0.783^{+0.021}_{-0.025}$ within the ΛCDM framework (Abbott et al. 2018). This value differs from the S_8 inferred in the 12-parameter model with CMB+BAO and CMB+BAO+SNe by only ~ 0.5–0.6σ, as can be read from Table 2. Hence, no significant S_8 tension is present, and the WL data can be consistently combined with the CMB+BAO or CMB+BAO+SNe datasets considered in this work. We further note that cosmological probes independent of both CMB and weak lensing also favor slightly lower values of S_8 compared to the CMB (see, e.g., Silva & Nunes (2025), which combines DESI DR2 BAO with the SDSS BOSS DR12 full-shape power spectrum). This suggests that the S_8 values inferred from weak lensing measurements may indeed be quite plausible.

Also, as noted previously in Roy Choudhury & Okumura (2024), the S_8 tension with DES Year 3 data is only at the level of 1.4σ (see also Tristram et al. (2024)), with DES Y3 preferring slightly lower values of S_8 compared to DES Y1 (Abbott et al. 2022). Consequently, had we adopted the DES Y3 likelihoods, we would likely have found stronger evidence for the lensing anomaly. It is important to remark, however, that recent results from the completed KiDS survey yield somewhat higher values of S_8, reporting $S_8 = 0.815^{+0.016}_{-0.021}$ within the ΛCDM framework (Wright et al. 2025). Thus, it remains unclear whether a $> 3\sigma$ lensing anomaly would persist when employing the KiDS dataset. Nevertheless, caution is necessary, since the model favored by the DESY5 SN data departs significantly from the standard ΛCDM scenario, and thus the S_8 constraints inferred from KiDS may also shift accordingly. And even without the WL data, our results are still significant, i.e., a 2σ+ lensing anomaly with CMB+BAO+SNe.

3.3. $\sum m_\nu$, $N_{\rm eff}$, *and* H_0

Figure 4 shows the probability posterior distributions of $\sum m_\nu$, $N_{\rm eff}$, and H_0. We find that the bounds on $\sum m_\nu$ are tighter than in the case where the full range of DE EoS parameters was allowed, as shown in our recent study Roy Choudhury (2025). This behavior is expected from the well-known geometric degeneracy between the DE EoS and $\sum m_\nu$, first noted in Hannestad (2005). In particular, models with $w(z) < -1$ tend to prefer larger neutrino masses, while scenarios with $w(z) > -1$ can yield bounds stronger than those obtained in ΛCDM Vagnozzi et al. (2018); Roy Choudhury & Naskar (2019). As illustrated in Figure 3 of Roy Choudhury (2025), the w_a parameter is strongly correlated with $\sum m_\nu$. In the present analysis, however, we do not obtain bounds stronger than ΛCDM, since we also vary $A_{\rm lens}$, which is itself strongly positively correlated with $\sum m_\nu$ Roy Choudhury & Hannestad (2020); higher $A_{\rm lens}$ values therefore drive larger neutrino mass estimates. Moreover, the inclusion of WL data slightly relaxes the bounds on $\sum m_\nu$, reflecting the strong negative correlation between S_8 and $\sum m_\nu$: larger neutrino masses enhance the suppression of the small-scale matter power spectrum, thereby lowering S_8.

We find that all dataset combinations yield slightly higher values of $N_{\rm eff}$, excluding the standard model prediction of $N_{\rm eff} = 3.044$ at more than 1σ but less than 2σ, indicating no statistically significant deviation. We also observe that the Hubble tension persists at the ~ 3.0–3.7σ level, depending on the dataset combination. At the two extreme ends, we find $H_0 = 68.5 \pm 1.1$ km/s/Mpc with CMB+DESI+WL, and $H_0 = 67.79 \pm 0.97$ km/s/Mpc with CMB+DESI+DESY5+WL. Hence, the tension remains robust, and the extensions explored in this work are insufficient to resolve it, pointing instead toward the need for new physics.

We note that it is well established that $N_{\rm eff}$ and H_0 are positively correlated (see, for instance, the rightmost panel of Figure 6 in Roy Choudhury (2025)). As discussed in the Introduction, an increase in $N_{\rm eff}$ enhances the radiation energy density in the early Universe, leading to a faster pre-recombination expansion rate and consequently a higher value of H_0. Interestingly, within the NPDDE framework, we obtain slightly larger values of $N_{\rm eff}$—and correspondingly higher H_0—than in the dynamical dark energy scenario with the full allowed range of (w_0, w_a) (see Table 2 and compare with Table 2 of Roy Choudhury (2025)). This outcome is somewhat non-trivial, given that phantom dark energy is generally expected to drive a higher expansion rate and thus a larger H_0.

Also, a higher value of $N_{\rm eff}$ leads to an enhanced suppression of the CMB temperature and polarization power spectra (Baumann 2018; Baumann et al. 2019). This effect can be partially compensated by increasing n_s and α_s, resulting in a positive correlation of $N_{\rm eff}$ with both parameters. Consequently, we obtain slightly higher values of n_s and α_s compared to those reported in Roy Choudhury (2025), where the full parameter range of dynamical dark energy was allowed. This behavior may have implications for the viability of various inflationary models (Gerbino et al. 2017; Roy Choudhury et al. 2022). However, we find that $N_{\rm eff}$ and α_s are not correlated with $A_{\rm lens}$; therefore, our main conclusion regarding the lensing anomaly remains unaffected by variations in these parameters.

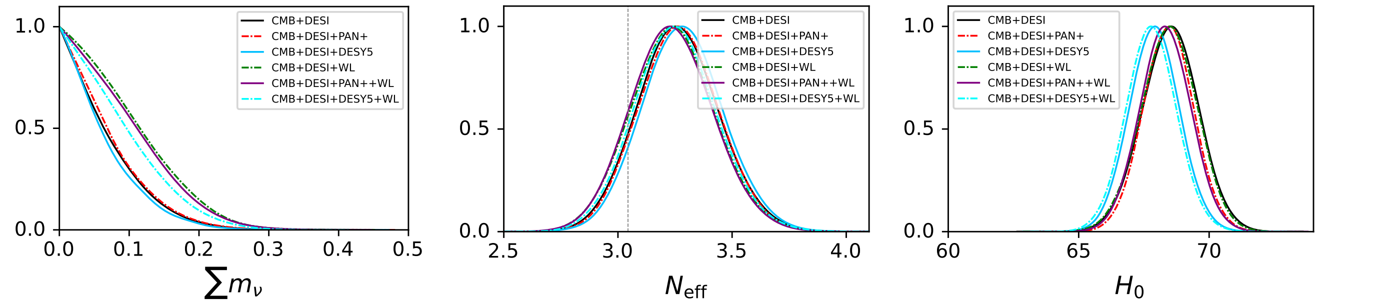

Figure 4. The left, middle, and right panels show the 1D posterior distributions of $\sum m_\nu$, $N_{\rm eff}$, and H_0 (km/s/Mpc) respectively, for various data combinations. The dashed vertical line in the middle panel corresponds to the standard model value of $N_{\rm eff} = 3.044$.

4. CONCLUSIONS

In this work, we have investigated an extended 12-parameter cosmological framework that incorporates non-phantom dynamical dark energy (NPDDE) in a spatially flat cosmology. By construction, this framework enforces the physically motivated condition that the dark energy equation of state (EoS) remains non-phantom at all times, i.e., $w(z) \geq -1$ for the entire cosmic history. This restriction ensures consistency with the class of quintessence-like models based on single scalar-field dynamics, thereby avoiding theoretical pathologies commonly associated with phantom scenarios. The parameter space we consider extends the standard six parameters of the ΛCDM model by including the dynamical dark energy parameters (w_0, w_a), the scaling of the CMB lensing amplitude $(A_{\rm lens})$, the sum of neutrino masses $(\sum m_\nu)$, the effective number of relativistic species $(N_{\rm eff})$, and the running of the scalar spectral index (α_s).

To constrain this model, we employed a comprehensive combination of state-of-the-art cosmological datasets. In particular, we used Baryon Acoustic Oscillation (BAO) measurements from the Dark Energy Spectroscopic Instrument (DESI) Data Release 2, CMB temperature and polarization spectra from Planck Public Release (PR) 4, CMB lensing from both Planck PR4 and Atacama Cosmology Telescope Data Release 6, uncalibrated Type Ia supernovae (SNe) data from the Pantheon+ and Dark Energy Survey Year 5 (DESY5) samples, and weak lensing (WL) data from DES Year 1. This joint analysis leverages the complementary constraining power of geometrical probes, cosmic shear measurements, and high-precision CMB data, thereby enabling us to test the viability of NPDDE models within a significantly enlarged cosmological parameter space.

Our key result is the robust detection of a lensing anomaly at greater than 3σ significance when combining CMB+BAO+WL data, as well as when extending the dataset combination to include SNe. Without the WL data, the significance of the lensing anomaly is still $2\sigma+$, even with Planck PR4 Hillipop+LoLLipop likelihoods which show agreement with the consistency-check parameter $A_{\rm lens} = 1$ at $< 1\sigma$ in ΛCDM. Specifically, we find that $A_{\rm lens}$ deviates from its theoretically expected value of unity, i.e., $A_{\rm lens} > 1$, indicating that the data prefer a higher level of CMB lensing than predicted by the NPDDE model. This result highlights a persistent tension: while our parameter space explicitly accommodates quintessence-like dark energy, doing so necessarily requires accepting the presence of a non-negligible lensing anomaly.

The implications of this finding are twofold. First, it strengthens the case that the lensing anomaly in a realistic Quintessence-like dark energy model is not an artifact of specific dataset choices, but instead emerges robustly when diverse probes are combined. Second, it suggests that models of quintessence-like dark energy cannot be evaluated in isolation: any consistent cosmological framework allowing for realistic dynamical dark energy must also contend with the presence of this anomaly. Possible explanations may include unresolved systematic effects in the datasets, unaccounted-for physical processes in the late universe, or extensions to the cosmological model that go beyond the NPDDE parameter space considered here.

Apart from the lensing anomaly, we find that the bounds on $\sum m_\nu$ are tighter than in scenarios where the full dark energy equation-of-state parameter space is allowed, reflecting the well-known degeneracy between neutrino mass and dark energy dynamics. Although models with $w(z) > -1$ can in principle yield bounds stronger than ΛCDM, our analysis does not achieve this once $A_{\rm lens}$ is varied, as it correlates positively with $\sum m_\nu$. The inclusion of weak lensing data further relaxes the bounds, owing to the negative correlation between S_8 and $\sum m_\nu$. Also, across all dataset combinations, we obtain mildly higher values of $N_{\rm eff}$, excluding the standard prediction at just above 1σ but below 2σ, without any statistically significant deviation. The Hubble tension remains at the ~ 3.0–3.7σ level depending on the dataset combination, indicating that the extensions explored here cannot resolve it and pointing instead toward the need for new physics.

Future work will benefit from upcoming high-precision datasets, particularly from CMB experiments such as Simons Observatory (Ade et al. 2019) and LiteBIRD (Campeti et al. 2024), further DESI releases, and large-scale galaxy clustering surveys (e.g., Vera Rubin Observatory (Ivezić et al. 2019) and Euclid (Amendola et al. 2018)). These will be crucial in clarifying whether the lensing anomaly persists at high statistical significance and in disentangling its physical origin. In this context, our results emphasize the importance of jointly analyzing dark energy phenomenology and secondary CMB anisotropy effects, since the viability of realistic quintessence models may ultimately hinge on the resolution of the lensing anomaly.

ACKNOWLEDGMENTS

We acknowledge the use of the HPC facility at ASIAA (https://hpc.tiara.sinica.edu.tw/) where the numerical analyses were done. SRC acknowledges support from grant No. I-IAA-ROY. TO acknowledges support from the Taiwan National Science and Technology Council of Taiwan under grants Nos. NSTC 112-2112-M-001-034-, NSTC 113-2112-M-001-011- and NSTC 114-2112-M-001-004-, and the Academia Sinica Investigator Project Grant No. AS-IV-114-M03 for the period of 2025–2029. KU acknowledges the support from grant Nos. AS-IA-112-M04, NSTC 112-2112-M-001-027-MY3, and I-SuMIRe.

REFERENCES

Abbott, T. M. C., et al. 2018, Phys. Rev. D, 98, 043526
—. 2022, Phys. Rev. D, 105, 023520
—. 2024, arXiv:2401.02929
Abdul Karim, M., et al. 2025, arXiv:2503.14738
Adam, H., Hertzberg, M. P., Jiménez-Aguilar, D., & Khan, I. 2025, arXiv:2509.13302
Adame, A. G., et al. 2024a, arXiv:2404.03002
—. 2024b, arXiv:2411.12022
Ade, P., et al. 2019, JCAP, 02, 056
Aghanim, N., et al. 2020a, Astron. Astrophys., 641, A1
—. 2020b, Astron. Astrophys., 641, A6, [Erratum: Astron.Astrophys. 652, C4 (2021)]
Akita, K., Hamaguchi, K., & Ovchynnikov, M. 2025, arXiv:2507.20659
Akrami, Y., Alestas, G., & Nesseris, S. 2025, arXiv:2504.04226
Akrami, Y., Sasaki, M., Solomon, A. R., & Vardanyan, V. 2021, Phys. Lett. B, 819, 136427
Akrami, Y., et al. 2020, Astron. Astrophys., 643, A42
Amendola, L. 2000, Phys. Rev. D, 62, 043511
Amendola, L., et al. 2018, Living Rev. Rel., 21, 2
An, H., Han, C., & Zhang, B. 2025, arXiv:2506.10075
Archidiacono, M., Hannestad, S., & Lesgourgues, J. 2020, JCAP, 09, 021
Arora, S., De Felice, A., & Mukohyama, S. 2025, arXiv:2508.03784
Banerjee, A., Cai, H., Heisenberg, L., et al. 2021, Phys. Rev. D, 103, L081305
Barua, S., & Desai, S. 2025, arXiv:2508.16238
Baumann, D. 2018, PoS, TASI2017, 009
Baumann, D., Beutler, F., Flauger, R., et al. 2019, Nature Phys., 15, 465
Bayat, Z., & Hertzberg, M. P. 2025, JCAP, 08, 065
Berghaus, K. V., Kable, J. A., & Miranda, V. 2024, Phys. Rev. D, 110, 103524
Bertólez-Martínez, T., Esteban, I., Hajjar, R., Mena, O., & Salvado, J. 2024, arXiv:2411.14524
Bhattacharya, S., Borghetto, G., Malhotra, A., et al. 2024, JCAP, 09, 073
—. 2025, JCAP, 04, 086
Borghetto, G., Malhotra, A., Tasinato, G., & Zavala, I. 2025, Phys. Rev. D, 112, 023521
Bostan, N., & Roy Choudhury, S. 2024, JCAP, 07, 032
Braglia, M., Chen, X., & Loeb, A. 2025, arXiv:2507.13925
Brooks, S. P., & Gelman, A. 1998, Journal of Computational and Graphical Statistics, 7, 434
Brout, D., et al. 2022, Astrophys. J., 938, 110
Cai, Y.-F., Saridakis, E. N., Setare, M. R., & Xia, J.-Q. 2010, Phys. Rept., 493, 1
Calabrese, E., Slosar, A., Melchiorri, A., Smoot, G. F., & Zahn, O. 2008, Phys. Rev. D, 77, 123531
Caldwell, R. R., Kamionkowski, M., & Weinberg, N. N. 2003, Phys. Rev. Lett., 91, 071301
Caldwell, R. R., & Linder, E. V. 2005, Phys. Rev. Lett., 95, 141301
Campeti, P., et al. 2024, JCAP, 06, 008
Carloni, Y., Luongo, O., & Muccino, M. 2025, Phys. Rev. D, 111, 023512

Carron, J., Mirmelstein, M., & Lewis, A. 2022, JCAP, 09, 039
Chakraborty, A., Chanda, P. K., Das, S., & Dutta, K. 2025, arXiv:2503.10806
Chakraborty, A., Ray, T., Das, S., Banerjee, A., & Ganesan, V. 2024, arXiv:2403.14247
Chaudhary, H., Capozziello, S., Praharaj, S., Pacif, S. K. J., & Mustafa, G. 2025a, arXiv:2509.17124
Chaudhary, H., Capozziello, S., Sharma, V. K., Gómez-Vargas, I., & Mustafa, G. 2025b, arXiv:2508.10514
Chaudhary, H., Capozziello, S., Sharma, V. K., & Mustafa, G. 2025c, arXiv:2507.21607
Chen, R., Cline, J. M., Muralidharan, V., & Salewicz, B. 2025, arXiv:2508.19101
Chen, S.-F., & Zaldarriaga, M. 2025, JCAP, 08, 014
Cheng, H., Di Valentino, E., Escamilla, L. A., Sen, A. A., & Visinelli, L. 2025, JCAP, 09, 031
Chevallier, M., & Polarski, D. 2001, Int. J. Mod. Phys. D, 10, 213
Choudhury, S. R., Hannestad, S., & Tram, T. 2021, J. Phys. Conf. Ser., 2156, 012016
Chung, D. J. H., Shiu, G., & Trodden, M. 2003, Phys. Rev. D, 68, 063501
Colgáin, E. Ó., Dainotti, M. G., Capozziello, S., et al. 2026, JHEAp, 49, 100428
Colgáin, E. O., Pourojaghi, S., Sheikh-Jabbari, M. M., & Yin, L. 2025, arXiv:2504.04417
Cortês, M., & Liddle, A. R. 2024, JCAP, 12, 007
Croker, K. S., Tarlé, G., Ahlen, S. P., et al. 2024, JCAP, 10, 094
Di Valentino, E., Gariazzo, S., & Mena, O. 2021, Phys. Rev. D, 104, 083504
Di Valentino, E., Melchiorri, A., Linder, E. V., & Silk, J. 2017, Phys. Rev. D, 96, 023523
Di Valentino, E., Melchiorri, A., & Silk, J. 2015, Phys. Rev. D, 92, 121302
—. 2016, Phys. Lett. B, 761, 242
—. 2019, Nature Astron., 4, 196
—. 2020, JCAP, 01, 013
Dinda, B. R., & Maartens, R. 2025a, JCAP, 01, 120
—. 2025b, Mon. Not. Roy. Astron. Soc., 542, L31
Dinda, B. R., Maartens, R., & Clarkson, C. 2025, arXiv:2509.19899
Easther, R., & Peiris, H. 2006, JCAP, 09, 010
Efstathiou, G. 2025, Mon. Not. Roy. Astron. Soc., 538, 875
Elbers, W., Frenk, C. S., Jenkins, A., Li, B., & Pascoli, S. 2025, Phys. Rev. D, 111, 063534
Eskilt, J. R., Akrami, Y., Solomon, A. R., & Vardanyan, V. 2022, Phys. Rev. D, 106, 023512
Esteban, I., Gonzalez-Garcia, M. C., Maltoni, M., Schwetz, T., & Zhou, A. 2020, JHEP, 09, 178
Fang, W., Hu, W., & Lewis, A. 2008, Phys. Rev. D, 78, 087303
Farrar, G. R., & Peebles, P. J. E. 2004, Astrophys. J., 604, 1
Fazzari, E., Giarè, W., & Di Valentino, E. 2025, arXiv:2509.16196
Feng, B., Wang, X.-L., & Zhang, X.-M. 2005, Phys. Lett. B, 607, 35
Feng, L., Han, T., Zhang, J.-F., & Zhang, X. 2025, arXiv:2507.17315
Gao, Q., Peng, Z., Gao, S., & Gong, Y. 2025a, Universe, 11, 10
Gao, S., Gao, Q., Gong, Y., & Lu, X. 2025b, Sci. China Phys. Mech. Astron., 68, 280408
Garcia-Bellido, J., & Roest, D. 2014, Phys. Rev. D, 89, 103527
García Escudero, H., Mirpoorian, S. H., & Pogosian, L. 2025, arXiv:2509.16202
Gariazzo, S., et al. 2022, JCAP, 10, 010
Gerbino, M., Freese, K., Vagnozzi, S., et al. 2017, Phys. Rev. D, 95, 043512
Gialamas, I. D., Hütsi, G., Kannike, K., et al. 2025a, Phys. Rev. D, 111, 043540
Gialamas, I. D., Hütsi, G., Raidal, M., et al. 2025b, Phys. Rev. D, 112, 063551
Giani, L., Von Marttens, R., & Piattella, O. F. 2025, arXiv:2505.08467
Giarè, W. 2025, Phys. Rev. D, 112, 023508
Giarè, W., Mahassen, T., Di Valentino, E., & Pan, S. 2025, Phys. Dark Univ., 48, 101906
Giarè, W., Mena, O., Specogna, E., & Di Valentino, E. 2025, arXiv:2507.01848
Giarè, W., Najafi, M., Pan, S., Di Valentino, E., & Firouzjaee, J. T. 2024, JCAP, 10, 035
Giusarma, E., Vagnozzi, S., Ho, S., et al. 2018, Phys. Rev. D, 98, 123526
Goldstein, S., Celoria, M., & Schmidt, F. 2025, arXiv:2507.16970
Guedezounme, S. L., Dinda, B. R., & Maartens, R. 2025, arXiv:2507.18274
Guo, Z.-K., Piao, Y.-S., Zhang, X.-M., & Zhang, Y.-Z. 2005, Phys. Lett. B, 608, 177
Handley, W. 2021, Phys. Rev. D, 103, L041301
Hannestad, S. 2005, Phys. Rev. Lett., 95, 221301
Herold, L., & Kamionkowski, M. 2025, Phys. Rev. D, 111, 083518
Herold, L., & Karwal, T. 2025, arXiv:2506.12004
Högås, M., & Mörtsell, E. 2025, arXiv:2507.03743

Hossain, M. W., & Maqsood, A. 2025, Phys. Rev. D, 112, 083504
Howlett, C., Lewis, A., Hall, A., & Challinor, A. 2012, JCAP, 04, 027
Huang, L., Cai, R.-G., & Wang, S.-J. 2025, Sci. China Phys. Mech. Astron., 68, 100413
Huang, Z. 2025, arXiv:2509.09086
Ishak, M., & Medina-Varela, L. 2025, arXiv:2507.22856
Ivezić, Ž., et al. 2019, Astrophys. J., 873, 111
Jhaveri, T., Karwal, T., & Hu, W. 2025, Phys. Rev. D, 112, 043541
Jiang, J.-Q., Pedrotti, D., da Costa, S. S., & Vagnozzi, S. 2024, Phys. Rev. D, 110, 123519
Jiang, J.-Q., Giarè, W., Gariazzo, S., et al. 2025, JCAP, 01, 153
Kessler, D. A., Escamilla, L. A., Pan, S., & Di Valentino, E. 2025, arXiv:2504.00776
Knox, L., & Millea, M. 2020, Phys. Rev. D, 101, 043533
Kohri, K., & Matsuda, T. 2015, JCAP, 02, 019
Kou, R., & Lewis, A. 2025, arXiv:2509.16155
Lee, B.-H., Lee, W., Colgáin, E. Ó., Sheikh-Jabbari, M. M., & Thakur, S. 2022, JCAP, 04, 004
Lee, D. H., Yang, W., Di Valentino, E., Pan, S., & van de Bruck, C. 2025, arXiv:2507.11432
Lee, S. 2025, arXiv:2505.19052
Lesgourgues, J., & Pastor, S. 2012, Adv. High Energy Phys., 2012, 608515
Lewis, A. 2019, arXiv:1910.13970
Lewis, A., Challinor, A., & Lasenby, A. 2000, Astrophys. J., 538, 473
Li, J.-X., & Wang, S. 2025, arXiv:2506.22953
Li, T.-N., Du, G.-H., Li, Y.-H., et al. 2025a, arXiv:2501.07361
Li, T.-N., Du, G.-H., Wu, P.-J., et al. 2025b, arXiv:2507.13811
Li, T.-N., Wu, P.-J., Du, G.-H., et al. 2024, Astrophys. J., 976, 1
—. 2025c, Phys. Dark Univ., 50, 102068
Linder, E. V. 2003, Phys. Rev. Lett., 90, 091301
—. 2008, Gen. Rel. Grav., 40, 329
Liu, T., Li, X., Xu, T., Biesiada, M., & Wang, J. 2025, arXiv:2507.04265
Lodha, K., et al. 2025a, Phys. Rev. D, 111, 023532
—. 2025b, arXiv:2503.14743
Luciano, G. G., & Paliathanasis, A. 2025, arXiv:2509.17527
Luciano, G. G., Paliathanasis, A., & Saridakis, E. N. 2026, JHEAp, 49, 100427
Luongo, O., & Muccino, M. 2025, Astron. Astrophys., 693, A187
MacCrann, N., et al. 2024, Astrophys. J., 966, 138
Madhavacheril, M. S., et al. 2024, Astrophys. J., 962, 113
Mazumdar, R., Gohain, M. M., & Bhuyan, K. 2025, arXiv:2507.05975
Meetei, E. C., & Singh, S. S. 2025, arXiv:2508.15187
Mirpoorian, S. H., Jedamzik, K., & Pogosian, L. 2025, arXiv:2504.15274
Mishra, S. S., Matthewson, W. L., Sahni, V., Shafieloo, A., & Shtanov, Y. 2025, arXiv:2507.07193
Moffat, J. W., & Thompson, E. J. 2025, arXiv:2505.18900
Mukherjee, P., & Sen, A. A. 2024, Phys. Rev. D, 110, 123502
—. 2025, arXiv:2505.19083
Nesseris, S., & Perivolaropoulos, L. 2004, Phys. Rev. D, 70, 123529
Nojiri, S., Odintsov, S. D., & Oikonomou, V. K. 2025, arXiv:2506.21010
Odintsov, S. D., Sáez-Chillón Gómez, D., & Sharov, G. S. 2025, Eur. Phys. J. C, 85, 298
Orchard, L., & Cárdenas, V. H. 2024, Phys. Dark Univ., 46, 101678
Özülker, E., Di Valentino, E., & Giarè, W. 2025, arXiv:2506.19053
Paliathanasis, A. 2025, Phys. Dark Univ., 48, 101956
Pang, Y.-H., Zhang, X., & Huang, Q.-G. 2025, Phys. Rev. D, 111, 123504
Park, C.-G., de Cruz Pérez, J., & Ratra, B. 2024, Phys. Rev. D, 110, 123533
—. 2025, Int. J. Mod. Phys. D, 34, 2550058
Park, C.-G., & Ratra, B. 2025a, Int. J. Mod. Phys. D, 34, 2550061
—. 2025b, arXiv:2501.03480
Payeur, G., McDonough, E., & Brandenberger, R. 2025, Phys. Rev. D, 111, 123541
Peng, Z.-Y., & Piao, Y.-S. 2025, Phys. Rev. D, 112, 023502
Petri, V., Marra, V., & von Marttens, R. 2025, arXiv:2508.17955
Plaza, F., León, G., & Kraiselburd, L. 2025, arXiv:2508.21175
Poulin, V., Boddy, K. K., Bird, S., & Kamionkowski, M. 2018, Phys. Rev. D, 97, 123504
Qiang, D.-C., Jia, J.-Y., & Wei, H. 2025, arXiv:2507.09981
Ramadan, O. F., Sakstein, J., & Rubin, D. 2024, Phys. Rev. D, 110, L041303
Rebouças, J., de Souza, D. H. F., Zhong, K., Miranda, V., & Rosenfeld, R. 2025, JCAP, 02, 024
Reeves, A., Herold, L., Vagnozzi, S., Sherwin, B. D., & Ferreira, E. G. M. 2023, Mon. Not. Roy. Astron. Soc., 520, 3688
Reeves, A., Nicola, A., & Refregier, A. 2025, JCAP, 06, 042
Riess, A. G., et al. 2022, Astrophys. J. Lett., 934, L7

Roy, N. 2025, Phys. Dark Univ., 48, 101912
Roy, N., & Chakrabarti, S. 2025, arXiv:2508.13740
Roy Choudhury, S. 2020, PhD thesis, HBNI, Mumbai
—. 2025, Astrophys. J. Lett., 986, L31
Roy Choudhury, S., & Choubey, S. 2018, JCAP, 09, 017
—. 2019, Eur. Phys. J. C, 79, 557
Roy Choudhury, S., & Hannestad, S. 2020, JCAP, 07, 037
Roy Choudhury, S., Hannestad, S., & Tram, T. 2021, JCAP, 03, 084
—. 2022, JCAP, 10, 018
Roy Choudhury, S., & Naskar, A. 2019, Eur. Phys. J. C, 79, 262
Roy Choudhury, S., & Okumura, T. 2024, Astrophys. J. Lett., 976, L11
Rubin, D., et al. 2023a, arXiv:2311.12098
—. 2023b, arXiv:2311.12098
Sanyal, A., & Rudra, P. 2025, arXiv:2508.19961
Scherer, M., Sabogal, M. A., Nunes, R. C., & De Felice, A. 2025, Phys. Rev. D, 112, 043513
Scolnic, D., et al. 2022, Astrophys. J., 938, 113
Shah, N., Koyama, K., & Noller, J. 2025, arXiv:2507.19450
Shao, H., Givans, J. J., Dunkley, J., et al. 2025, Phys. Rev. D, 111, 083535
Sharma, V. k., Chaudhary, H., & Kolekar, S. 2025, arXiv:2507.00835
Shim, J., Okumura, T., & Taruya, A. 2025, Astrophys. J. Lett., 985, L14
Shlivko, D., & Steinhardt, P. J. 2024, Phys. Lett. B, 855, 138826
Silva, E., & Nunes, R. C. 2025, arXiv:2507.13989
Silva, E., Sabogal, M. A., Scherer, M., et al. 2025, Phys. Rev. D, 111, 123511
Tada, Y., & Terada, T. 2024, Phys. Rev. D, 109, L121305
Tanseri, I., Hagstotz, S., Vagnozzi, S., Giusarma, E., & Freese, K. 2022, JHEAp, 36, 1
Toomey, M. W., Montefalcone, G., McDonough, E., & Freese, K. 2025, arXiv:2509.13318
Torrado, J., & Lewis, A. 2019, Cobaya: Bayesian analysis in cosmology, Astrophysics Source Code Library, record ascl:1910.019
Torrado, J., & Lewis, A. 2021, JCAP, 05, 057
Tristram, M., et al. 2024, Astron. Astrophys., 682, A37
Tsedrik, M., et al. 2025, arXiv:2502.03390
Vagnozzi, S. 2020, Phys. Rev. D, 102, 023518
—. 2023, Universe, 9, 393
Vagnozzi, S., Dhawan, S., Gerbino, M., et al. 2018, Phys. Rev. D, 98, 083501
Vagnozzi, S., Giusarma, E., Mena, O., et al. 2017, Phys. Rev. D, 96, 123503
van de Bruck, C., Mifsud, J., & Morrice, J. 2017, Phys. Rev. D, 95, 043513
van der Westhuizen, M., Abebe, A., & Di Valentino, E. 2025a, arXiv:2509.04495
—. 2025b, arXiv:2509.04494
—. 2025c, arXiv:2509.04496
van der Westhuizen, M., Figueruelo, D., Thubisi, R., et al. 2025d, arXiv:2505.23306
Vikman, A. 2005, Phys. Rev. D, 71, 023515
Wang, D., Mena, O., Di Valentino, E., & Gariazzo, S. 2025a, arXiv:2503.18745
Wang, H., & Piao, Y.-S. 2024, arXiv:2404.18579
—. 2025, arXiv:2506.04306
Wang, J.-Q., Cai, R.-G., Guo, Z.-K., & Wang, S.-J. 2025b, arXiv:2508.01759
Wang, Y., & Freese, K. 2025, arXiv:2505.17415
Wang, Y., & Tegmark, M. 2004, Phys. Rev. Lett., 92, 241302
Wang, Y.-Y., Lei, L., Tang, S.-P., & Fan, Y.-Z. 2025c, arXiv:2508.19081
Wolf, W. J., Ferreira, P. G., & García-García, C. 2025a, arXiv:2509.17586
Wolf, W. J., Ferreira, P. G., & García-García, C. 2025b, Phys. Rev. D, 111, L041303
Wolf, W. J., García-García, C., Bartlett, D. J., & Ferreira, P. G. 2024, Phys. Rev. D, 110, 083528
Wolf, W. J., García-García, C., & Ferreira, P. G. 2025c, JCAP, 05, 034
Wolf, W. J., & Read, J. 2025, arXiv:2501.13521
Wright, A. H., et al. 2025, arXiv:2503.19441
Wu, P.-J., Li, T.-N., Du, G.-H., & Zhang, X. 2025, arXiv:2509.02945
Yang, W., Nunes, R. C., Pan, S., & Mota, D. F. 2017, Phys. Rev. D, 95, 103522
Yang, W., Zhang, S., Mena, O., Pan, S., & Di Valentino, E. 2025a, arXiv:2508.19109
Yang, Y. 2025, arXiv:2508.17848
Yang, Y., Wang, Q., Li, C., et al. 2025b, JCAP, 08, 050
Ye, G. 2024, arXiv:2411.11743
Ye, G., & Cai, Y. 2025, arXiv:2503.22515
Ye, G., & Lin, S.-J. 2025, arXiv:2505.02207
Ye, G., Martinelli, M., Hu, B., & Silvestri, A. 2025, Phys. Rev. Lett., 134, 181002
Yin, W. 2024, JHEP, 05, 327
Zapata, M. A., Garcia-Arroyo, G., Adil, S. A., & Vazquez, J. A. 2025, arXiv:2507.22292
Zhou, S.-H., Li, T.-N., Du, G.-H., et al. 2025, arXiv:2509.10836
Zlatev, I., Wang, L.-M., & Steinhardt, P. J. 1999, Phys. Rev. Lett., 82, 896

Zuntz, J., Paterno, M., Jennings, E., et al. 2015, Astron. Comput., 12, 45